An Inelastic Damage Model for Fiber Reinforced Laminates

EVER J. BARBERO*
Mechanical and Aerospace Engineering
West Virginia University
Morgantown, WV 26506-6106, USA

PAOLO LONETTI
Department of Structural Engineering
University of Calabria
Italy

(Received December 12, 2000)
(Revised April 13, 2001)

ABSTRACT: A new model for damage behavior of polymer matrix composite laminates is presented. The model is developed for an individual lamina, and then assembled to describe the nonlinear behavior of the laminate. The model predicts the inelastic effects as reduction of stiffness and increments of damage and unrecoverable deformation. The model is defined using Continuous Damage Mechanics coupled with Classical Thermodynamic Theory. Unrecoverable deformations and Damage are coupled by the concept of effective stress. New expressions of damage and unrecoverable deformation domains are presented so that the number of model parameters is small. Furthermore, model parameters are obtained from existing test data for unidirectional laminae, supplemented by cyclic shear stress–strain data. Comparison with lamina and laminate test data are presented to demonstrate the ability of the model to predict the observed behavior.

INTRODUCTION

THE ADVANCING USE of polymer matrix composites (PMC) in applications with long life cycles requires better analysis techniques to predict material degradation and failure. Experimental results show marked nonlinear effects when a single lamina is loaded by shear [1,2]. Instead, lower nonlinearity appears when the loading is along the fiber direction or transverse to it. The most common modes of failure of PMCs are fiber breakage, fiber-matrix debonding, matrix cracks, and fiber kinking. Fabrication of PMCs inevitably creates body defects in the form of matrix cracks, voids, crazes, delaminations,

*Author to whom correspondence should be addressed. E-mail: ebarbero@wvu.edu.

0021-9983/02/08 0941–22 $10.00/0 DOI: 10.1106/002199802023549

fiber-matrix debond, and so on. The evolution of such defects influence stress–strain response of the laminae and the maximum load that a laminate can support. The present paper deals with Continuous Damage Mechanics of homogenized media where the effect of the constituents has been averaged. Therefore, the model cannot identify individual failure modes. The effect of the likely failure modes is felt in the damage measures d_{ii}, on an average sense only.

The proposed model is constructed coupling the damage and unrecoverable deformations theories using a thermodynamic formulation. A mesoscale approach is used, thus the constitutive equations refer to a single lamina of orthotropic material. The global behavior is determined assembling the contributions of each lamina using the classical laminate theory, modified for a continuously damaging material with plastic-like unrecoverable deformations. Damage and unrecoverable deformations surfaces are developed to accomplish good correlation with experimental observations while using a few adjustable parameters that have clear physical interpretation and are easy to determine from existing experimental data. The evolution laws are defined in standard and nonstandard formulation for unrecoverable deformations and damage respectively. The principle of maximum entropy is used in order to define the evolution of internal variables.

While several models are available to account damage and unrecoverable deformations effects for a lamina [3,4,6], the proposed model is defined in terms of fewer adjustable parameters. Furthermore, the parameters in the proposed model are evaluated from existing experimental data rather than from specialized, nonstandard tests. Although the model still contains five adjustable parameters, all of them can be determined from available experimental data. Experimental results for unidirectional laminae and laminates demonstrate the qualities of the proposed model.

DAMAGE DEFINITION

The damage definition due to Kachanov-Rabotnov is used [7,8]. The local density of defects is assumed uniformly distributed in a representative volume element. Lamina experimental results evidence different damage modes and evolution for longitudinal, transverse, and shear loading [1,2]. In addition, shear loading leads to longitudinal and mostly transverse damage [9–11]. Therefore, the orientation of defects is described by a second order tensor with principal directions coinciding with the material coordinate axes of the lamina.

The damage variables are (a) a second order symmetric damage tensor D, defined to account for the anisotropic evolution of defects along matrix and fiber directions and (b) a scalar damage hardening parameter δ that controls the size of the damage surface. The evolution law is assumed to be isotropic for simplicity and due to the lack of experimental observations indicating anisotropic evolution of the damage surface.

The unrecoverable deformation variables are (c) a second order symmetric tensor ε^p to account for the accumulated, unrecoverable deformations and (d) a scalar unrecoverable deformation hardening parameter p that controls the size of the unrecoverable deformation surface. The evolution law is assumed to be isotropic for simplicity and due to the lack of experimental observations indicating otherwise.

A diagonal second order tensor is chosen to describe the damage effects $D = [d_{11}, d_{22}, d_{33}]$, because it yields simplicity to the constitutive equations. A refined formulation could be obtained using a fourth order damage tensor [3,12,13] but it would result in greater complexity. The use of damage and integrity tensors describes a mapping between the effective $\overline{\mathbb{C}}$ and damaged $\mathbb{C}$ configurations by a unique transformation $\mathbb{C} \rightarrow \overline{\mathbb{C}}$. By the square root theorem [14,15], a unique transformation connects the damage and integrity tensor $\Omega = \sqrt{I - D}$. The eigenvalues of the damage tensor d_i represent the net area reduction along the principal axis, which coincide with the principal directions of the integrity tensor Ω. Experimental results on a single composite lamina show that during the deformation, microcracks, voids, and defects have preferential directions along which damage and unrecoverable deformation growth occurs. Since they typically coincide with material axes, it is assumed that the principal axes of the damage tensor D are aligned with the material axes and do not necessarily match the principal directions of stress. The effective stress is defined [16] as

$$\overline{\sigma} = M^{-1}(D)\sigma = (\Omega^{-1} \otimes \Omega^{-1})\sigma = \left[(\sqrt{1-D})^{-1} \otimes (\sqrt{1-D})^{-1}\right]\sigma \tag{1}$$

where M is a fourth order tensor called the damage effect tensor. By the symmetry of the σ and $\overline{\sigma}$ tensors, the damage effect tensor M is doubly symmetric. An explicit expression is then found in contracted notation [17] as

$$M_{ijkl} = \Omega_{ik}\Omega_{lj} \begin{bmatrix} \Omega_1^2 & 0 & 0 & 0 & 0 & 0 \\ & \Omega_2^2 & 0 & 0 & 0 & 0 \\ & & \Omega_3^2 & 0 & 0 & 0 \\ & & & \dfrac{\Omega_3\Omega_2}{2} & 0 & 0 \\ & \text{sym} & & & \dfrac{\Omega_1\Omega_3}{2} & 0 \\ & & & & & \dfrac{\Omega_1\Omega_2}{2} \end{bmatrix} \tag{2}$$

In terms of Equation (2), Equation (1) reduces to the following explicit relationships

$$\overline{\sigma} = \begin{bmatrix} \dfrac{\sigma_{11}}{(1-d_1)} & \dfrac{\sigma_{12}}{\sqrt{(1-d_1)(1-d_2)}} & 0 \\ \text{sym} & \dfrac{\sigma_{22}}{(1-d_2)} & 0 \\ 0 & 0 & 0 \end{bmatrix}$$

$$\overline{\varepsilon}' = \begin{bmatrix} \varepsilon'_{11}(1-d_1) & \varepsilon'_{12}\sqrt{(1-d_1)(1-d_2)} & 0 \\ \text{sym} & \varepsilon'_{22}(1-d_2) & 0 \\ 0 & 0 & 0 \end{bmatrix} \tag{3}$$

where prime indicates the elastic, recoverable part of the strain.

CONSTITUTIVE MODEL

General coupled elastoplastic and damage theory [18–20] allows us to write the total strain tensor ε as sum of unrecoverable and elastic strains. The inelastic process is modeled introducing a set of internal variables that describes the unrecoverable and damage behavior of the material. The Helmholtz free energy is a function of internal variables, elastic strain, and temperature. The Helmholtz free energy is postulated to be sum of two terms, the strain energy $\varphi(\varepsilon, \varepsilon^p, D)$ and the dissipation energy $\pi(p, \delta)$ [5;6]

$$\psi = \psi(\varepsilon, \varepsilon^p, p, D, \delta) = \varphi(\varepsilon, \varepsilon^p, D) + \pi(p, \delta) \tag{4}$$

where ε^p, D are the unrecoverable strain and damage second order tensors and p, δ are the hardening parameters. The strain energy can be assumed to be

$$\varphi(\varepsilon, \varepsilon^p, D) = \frac{1}{2}(\varepsilon - \varepsilon^p)E(D)(\varepsilon - \varepsilon^p) \tag{5}$$

where the $E(D)$ is a fourth order tensor that expresses the damaged stiffness of the material. The damaged stiffness tensor is defined according to the principle of equivalent elastic energy [21,22], which states that the elastic energy of the damaged material is the same in form as that of an effective material except that the stress tensor is replaced by the effective stress

$$\varphi(\overline{\sigma}, 0) = \frac{1}{2}\sigma(E)^{-1}\sigma = \frac{1}{2}\overline{\sigma}(\overline{E})^{-1}\overline{\sigma} = \frac{1}{2}\sigma M^{-1}(\overline{E})^{-1}M^{-1}\sigma \tag{6}$$

The damage stiffness tensor is written in terms of the effective stiffness tensor $E = M\overline{E}M$, which is a fourth order tensor, quadratic in the damage variable D. In terms of Equation (2), we get the stiffness tensor explicitly as

$$E(D) = \begin{bmatrix} \overline{E}_{11}(1-d_1)^2 & \overline{E}_{12}(1-d_1)(1-d_2) & 0 & 0 & 0 & 0 \\ & \overline{E}_{22}(1-d_2)^2 & 0 & 0 & 0 & 0 \\ & & 0 & 0 & 0 & 0 \\ & & & 0 & 0 & 0 \\ & \text{sym} & & & 0 & 0 \\ & & & & & \frac{1}{2}\overline{E}_{66}(1-d_1)(1-d_2) \end{bmatrix} \tag{7}$$

and the compliance tensor as $C = E^{-1}$. The dissipation energy $\pi(p, \delta)$ can be separated into two terms, which express the evolution of the damage and unrecoverable deformation surfaces

$$\pi(p, \delta) = R(p) + \gamma(\delta) \tag{8}$$

Here, we postulate that

$$R(p) = -\frac{1}{2}c_1^p p^2 \tag{9}$$

and

$$\gamma(\delta) = c_1 \exp\left[\frac{\delta}{c_2}\right] \tag{10}$$

where c_1^p, c_1, c_2 are material parameters. Since the function $\pi(p,\delta)$ is assumed to be convex, its second derivative must be positive. Therefore, the material constants must satisfy the following conditions $c_1 > 0$; $c_2 < 0$; $c_1^p > 0$ [23]. The conjugate thermodynamic forces associated to the cinematic variables $(\varepsilon, \varepsilon^p, p, D, \delta)$ are

$$
\begin{aligned}
\sigma &= -\frac{\partial\psi}{\partial\varepsilon} = E(D)(\varepsilon - \varepsilon^p) \\
Y &= -\frac{\partial\psi}{\partial D} = -\frac{1}{2}(\varepsilon - \varepsilon^p)\frac{\partial}{\partial D}[ME(D)M](\varepsilon - \varepsilon^p) \\
R &= -\frac{\partial\psi}{\partial p} = -c_1^p p \\
\gamma &= -\frac{\partial\psi}{\partial\delta} = c_1^d \exp\left(\frac{\delta}{c_2^d}\right)
\end{aligned}
\tag{11}
$$

Using Equation (7), explicit expressions for the thermodynamic forces are found as

$$
\begin{aligned}
Y_1 &= \frac{1}{\Omega_1^2}(\overline{E_{11}\varepsilon_1'^2} + \overline{E_{12}\varepsilon_1'\varepsilon_2'} + \overline{E_{66}\varepsilon_{12}'^2}) = \frac{1}{\Omega_1^2}(\overline{C_{11}\sigma_1^2} + \overline{C_{12}\sigma_1\sigma_2} + \overline{C_{66}\sigma_6^2}) \\
Y_2 &= \frac{1}{\Omega_2^2}(\overline{E_{22}\varepsilon_1'^2} + \overline{E_{12}\varepsilon_1'\varepsilon_2'} + \overline{E_{66}\varepsilon_{12}'^2}) = \frac{1}{\Omega_2^2}(\overline{C_{22}\sigma_2^2} + \overline{C_{12}\sigma_1\sigma_2} + \overline{C_{66}\sigma_6^2}) \\
\varepsilon' &= \varepsilon - \varepsilon^p
\end{aligned}
\tag{12}
$$

and $Y_3 = 0$ for a state of plane stress. Considering the principle of maximum entropy [24] and using the Lagrange minimization method the evolution equations can be defined as

$$
\begin{aligned}
\dot{\overline{\varepsilon^p}} &= \dot{\lambda}^p \frac{\partial g^p}{\partial\overline{\sigma}}; \quad \dot{p} = \dot{\lambda}^p \frac{\partial g^p}{\partial R} \\
\dot{D} &= \dot{\lambda}^d \frac{\partial f^d}{\partial Y}; \quad \dot{\delta} = \dot{\lambda}^d \frac{\partial f^d}{\partial\gamma}
\end{aligned}
\tag{13}
$$

where $\dot{\lambda}^p$, $\dot{\lambda}^d$ are the damage and unrecoverable deformations multipliers, g^p, f^d are the dissipation potentials. In addition, the unloading conditions follow directly from the Kuhn–Tucker optimality conditions [24] as

$$
\begin{aligned}
\dot{\lambda}^p \geq 0; &\quad \dot{\lambda}^d \geq 0 \\
g^p \leq 0; &\quad g^d \leq 0 \\
g^p\dot{\lambda}^p = 0; &\quad g^d\dot{\lambda}^d = 0
\end{aligned}
\tag{14}
$$

DAMAGE DOMAIN

Next, the damage surface and the dissipation potential are written in the thermodynamic variables domain Y_i, which in thermodynamic sense are the conjugate variables of the damage tensor D [23]. The damage surface limits the state for which the material experiences no damage. A nonstandard formulation is then used to define the damage function g^d and potential surface f^d as

$$
\begin{aligned}
g^d &= g(Y) - \gamma(\delta) - \gamma_0 = \sqrt{Y - J \cdot Y} + \sqrt{|H \cdot Y|} - (\gamma(\delta) + \gamma_0) \\
f^d &= f(Y) - \gamma(\delta) - \gamma_0 = \sqrt{Y - J \cdot Y} - (\gamma(\delta) + \gamma_0)
\end{aligned} \tag{15}
$$

where **J** and **H** are fourth and second order tensors respectively, γ_0 is the damage energy threshold. The tensors **J** and **H** are material dependent. It is worth noting that the linear term in Equation (15) allows us to take into account different behavior of the composite lamina in tension and compression. The coefficients in the tensors **J** and **H** are univocally determined in terms of material properties as explained in section Internal Material Constants. The damage domain surface g^d in Equation (15) has the shape of the Tsai–Wu surface when the first of Equation (15) is written in stress space [23]

$$
\begin{aligned}
& g(\bar{\sigma}) = f_1\bar{\sigma}_1 + f_2\bar{\sigma}_2 + f_{11}\bar{\sigma}_1^2 + f_{22}\bar{\sigma}_2^2 + 2f_{12}\bar{\sigma}_1\bar{\sigma}_2 + f_{66}\bar{\sigma}_6^2 - (\gamma(\delta) + \gamma_0) \\
& f_1 = \frac{1}{F_{1t}} - \frac{1}{F_{1c}}; \quad f_2 = \frac{1}{F_{2t}} - \frac{1}{F_{2c}}; \quad f_{11} = \frac{1}{F_{1t}F_{1t}} \\
& f_{22} = \frac{1}{F_{2t}F_{2t}}; \quad f_{66} = \frac{1}{F_6^2}; \quad f_{12} \cong -\frac{0.5}{F_{1t}^2}
\end{aligned} \tag{16}
$$

The Tsai–Wu criterion is recovered when the last term on the right hand side is set to one. The magnitude of the last term affects the size of the damage surface but its shape remains similar to that of a Tsai–Wu surface. Since the Tsai–Wu criterion predicts ply failure, the damage surface coincides with ply failure when the last term is equal to one. Then $\gamma(\delta) = 0$, the last terms reduces to γ_0. Thus, the initial size of the surface Equation (16) is smaller and it represents the loci of stress at which damage starts. For the sake of simplicity, it is assumed that the shape of the damage domain remains the same while its size grows until it reaches the Tsai–Wu criterion at ply failure.

The evolution of the damage is governed by a hardening function that involves two variables c_1, c_2, which are material dependent. The proposed damage hardening function is given by Equation (10). The consistency condition ($\dot{g}^d = g^d = 0$), and the normality rule Equation (13), used in the CDM framework [25,26] allows us to derive the following equation in terms of the damage and unrecoverable deformation multipliers $\dot{\lambda}^d$, $\dot{\lambda}^p$, using

$$
\begin{aligned}
& \frac{\partial g^d}{\partial Y} Y + \frac{\partial g^d}{\partial \gamma}\dot{\gamma} = 0; \quad \bar{\sigma} = M^{-1}\sigma; \quad \dot{\varepsilon} = M^{-1}\dot{\bar{\varepsilon}} \\
& Y = \frac{\partial Y}{\partial \varepsilon}\dot{\varepsilon} + \frac{\partial Y}{\partial \varepsilon^p}\dot{\varepsilon}^p + \frac{\partial Y}{\partial D}\dot{D} = \frac{\partial Y}{\partial \varepsilon}\dot{\varepsilon} + \frac{\partial Y}{\partial \varepsilon^p} M^{-1}\dot{\bar{\varepsilon}}^p + \frac{\partial Y}{\partial D}\dot{D} \\
& \quad = \frac{\partial Y}{\partial \varepsilon}\dot{\varepsilon} + \frac{\partial Y}{\partial \varepsilon^p} M^{-1}\dot{\lambda}^p \frac{\partial g^p}{\partial \bar{\sigma}} + \frac{\partial Y}{\partial D}\dot{\lambda}^d \frac{\partial f^d}{\partial D} \\
& \dot{g}^d = \frac{\partial g^d}{\partial Y}\left[\frac{\partial Y}{\partial \varepsilon}\dot{\varepsilon} + \frac{\partial Y}{\partial \varepsilon^p} M^{-1}\dot{\lambda}^p \frac{\partial g^p}{\partial \bar{\sigma}} + \frac{\partial Y}{\partial D}\dot{\lambda}^d \frac{\partial f^d}{\partial D}\right] + \frac{\partial g^d}{\partial \gamma}\frac{\partial \gamma}{\partial \delta}\dot{\lambda}^d \frac{\partial f^d}{\partial \gamma} = 0 \\
& \dot{g}^d = \dot{\lambda}^d\left[\frac{\partial g^d}{\partial Y}\frac{\partial Y}{\partial D}\frac{\partial f^d}{\partial D} + \frac{\partial g^d}{\partial \gamma}\frac{\partial \gamma}{\partial \delta}\frac{\partial f^d}{\partial \gamma}\right] + \frac{\partial g^d}{\partial Y}\frac{\partial Y}{\partial \varepsilon^p} M^{-1}\dot{\lambda}^p \frac{\partial g^p}{\partial \bar{\sigma}} + \frac{\partial g^d}{\partial Y}\frac{\partial Y}{\partial \varepsilon}\dot{\varepsilon} = 0
\end{aligned} \tag{17}
$$

UNRECOVERABLE DEFORMATIONS DOMAIN

Unrecoverable deformations of composite materials are more evident for shear loading than longitudinal and transverse loading [2]. The unrecoverable strain evolution is realized by the classical plasticity formulation [20]. The loading surface and the dissipation potential are identical in the effective stress space, thus following a standard formulation. A Tsai–Wu surface is chosen because of its ability to represent different behavior among the different load paths in stress space. Therefore, the loading surface used herein is

$$g^p = g(\overline{\sigma}) - R(p) - R_0 \tag{18}$$

where the unrecoverable deformation domain is defined in effective stress space as

$$\begin{aligned}
g(\overline{\sigma}) &= f_1\overline{\sigma}_1 + f_2\overline{\sigma}_2 + f_{11}\overline{\sigma}_1^2 + f_{22}\overline{\sigma}_2^2 + 2f_{12}\overline{\sigma}_1\overline{\sigma}_2 + f_{66}\overline{\sigma}_6^2 \\
f_1 &= \frac{1}{F_{1t}} - \frac{1}{F_{1c}}; \quad f_2 = \frac{1}{F_{2t}} - \frac{1}{F_{2c}}; \quad f_{11} = \frac{1}{F_{1t}F_{1t}} \\
f_{22} &= \frac{1}{F_{2t}F_{2t}}; \quad f_{66} = \frac{1}{F_6^2}; \quad f_{12} \cong -\frac{0.5}{F_{1t}^2}
\end{aligned} \tag{19}$$

and R_0 is the unrecoverable deformations threshold. The parameters F_i are material dependent and represent the strength values in tension, compression and shear for a single composite lamina. These values are tabulated in the literature [17,27], or they can be easily obtained following standardized test methods [28]. Unrecoverable deformation hardening is modeled by a simple function Equation (9), thus requiring the minimum number of internal parameters to describe it. As before, by the consistency condition ($g^p = \dot{g}^p = 0$), the normality evolution rules, and the effective stress concept, it is possible to obtain the following relations

$$\begin{gathered}
R(p) - K_p p; \quad \dot{\overline{\sigma}} = M^{-1}\sigma; \quad \dot{\varepsilon} = M^{-1}\dot{\overline{\varepsilon}} \\
\frac{\partial g^p}{\partial \overline{\sigma}}\dot{\overline{\sigma}} + \frac{\partial g^p}{\partial R}\dot{R} = 0 \\
\dot{\overline{\sigma}} = \frac{\partial \overline{\sigma}}{\partial \varepsilon}\dot{\varepsilon} + \frac{\partial \overline{\sigma}}{\partial \varepsilon^p}\dot{\varepsilon}^p + \frac{\partial \overline{\sigma}}{\partial D}\dot{D} = M^{-1}\frac{\partial \sigma}{\partial \varepsilon}\dot{\varepsilon} + M^{-1}\frac{\partial \sigma}{\partial \varepsilon^p}\dot{\varepsilon}^p + \frac{\partial}{\partial D}[M^{-1}\sigma]\dot{D} \\
\dot{\overline{\sigma}} = M^{-1}\frac{\partial \sigma}{\partial \varepsilon}\dot{\varepsilon} + M^{-1}\frac{\partial \sigma}{\partial \varepsilon^p}M^{-1}\dot{\lambda}^p\frac{\partial g^p}{\partial \overline{\sigma}} + \frac{\partial}{\partial D}[M^{-1}\sigma]\dot{\lambda}^d\frac{\partial f}{\partial D} \\
\dot{g}^p = \frac{\partial g^p}{\partial \overline{\sigma}}M^{-1}\frac{\partial \sigma}{\partial \varepsilon}\dot{\varepsilon} + M^{-1}\frac{\partial \sigma}{\partial \varepsilon^p}M^{-1}\dot{\lambda}^p\frac{\partial g^p}{\partial \overline{\sigma}} + \frac{\partial}{\partial D}[M^{-1}\sigma]\dot{\lambda}^d\frac{\partial f}{\partial D} = 0 \\
\frac{\partial g^p}{\partial \overline{\sigma}}M^{-1}\frac{\partial \sigma}{\partial \varepsilon}\dot{\varepsilon} + \frac{\partial g^p}{\partial \overline{\sigma}}M^{-1}\frac{\partial \sigma}{\partial \varepsilon^p}M^{-1}\dot{\lambda}^p\frac{\partial g^p}{\partial \overline{\sigma}} + \frac{\partial g^p}{\partial \overline{\sigma}}\frac{\partial}{\partial D}[M^{-1}\sigma]\dot{\lambda}^d\frac{\partial f}{\partial D} + \frac{\partial g^p}{\partial R}\frac{\partial R}{\partial p}\frac{\partial g^p}{\partial R} = 0 \\
\dot{\lambda}^p\left[\frac{\partial g^p}{\partial \overline{\sigma}}M^{-1}\frac{\partial \sigma}{\partial \varepsilon^p}M^{-1}\frac{\partial g^p}{\partial \overline{\sigma}} + \frac{\partial g^p}{\partial R}\frac{\partial R}{\partial p}\frac{\partial g^p}{\partial R}\right] + \dot{\lambda}^d\left[\frac{\partial g^p}{\partial \overline{\sigma}}\frac{\partial}{\partial D}[M^{-1}\sigma]\frac{\partial f}{\partial D}\right] + \frac{\partial g^p}{\partial \overline{\sigma}}M^{-1}\frac{\partial \sigma}{\partial \varepsilon}\dot{\varepsilon} = 0
\end{gathered} \tag{20}$$

in which the damage and unrecoverable deformation multipliers $\dot{\lambda}^p$, $\dot{\lambda}^d$ are the unknown quantities. Solving the linear system defined by Equations (17) and (20), it is possible to determine the values of $\dot{\lambda}^p$, $\dot{\lambda}^d$ which define the damage and unrecoverable deformations evolution laws.

LAMINATE MODEL

The model presented so far predicts the behavior of a single lamina. Classical laminate theory is used next to introduce the damage and unrecoverable effects in the constitutive equations for a laminate [17]. Damage and unrecoverable effects are introduced so that stress redistribution among various layers in a laminate is properly accounted for. The stress–strain relations in the material coordinates for the top or the bottom surface of a single lamina are

$$\begin{bmatrix} \sigma_1 \\ \sigma_2 \\ \sigma_3 \end{bmatrix}^{Z_k^t} = \begin{bmatrix} Q_{11}^d & Q_{12}^d & 0 \\ Q_{12}^d & Q_{22}^d & 0 \\ 0 & 0 & Q_{66}^d \end{bmatrix}^{Z_k^t} \begin{bmatrix} \varepsilon_1 - \varepsilon_1^p \\ \varepsilon_2 - \varepsilon_2^p \\ \gamma_6 - \gamma_6^p \end{bmatrix}^{Z_k^t};$$

$$\begin{bmatrix} \sigma_1 \\ \sigma_2 \\ \sigma_3 \end{bmatrix}^{Z_k^b} = \begin{bmatrix} Q_{11}^d & Q_{12}^d & 0 \\ Q_{12}^d & Q_{22}^d & 0 \\ 0 & 0 & Q_{66}^d \end{bmatrix}^{Z_k^b} \begin{bmatrix} \varepsilon_1 - \varepsilon_1^p \\ \varepsilon_2 - \varepsilon_2^p \\ \gamma_6 - \gamma_6^p \end{bmatrix}^{Z_k^b} \tag{21}$$

where the subscripts d, p, refer to damage and unrecoverable effects, respectively, and superscripts t, b refer to top and bottom, respectively. In the framework of the classical plate theory (CPT) the kinematic variables are the midplane strain and curvatures. The elastic-damaged terms of the reduced stiffness matrix are defined by a linear function of the material property of top and bottom surface of the kth lamina as

$$\overline{Q_{ij}^d}(z) = \overline{Q_{ij}^d}(Z_k^b) + \frac{\overline{Q_{ij}^d}(Z_k^t) - \overline{Q_{ij}^d}(Z_k^b)}{(Z_k^t - Z_k^b)}(z - Z_k^b) \tag{22}$$

where an overbar ($\bar{\ }$) indicates quantities in the global coordinate system of the laminate. Such quantities are obtained by standard coordinate transformation [17] of Equation (21). The tension σ_i over the lamina is a linear function of the top and bottom values of the stress, given by

$$\sigma_i(z) = \sigma_i(Z_k^b) + \frac{\sigma_i(Z_k^t) - \sigma_i(Z_k^b)}{(Z_k^t - Z_k^b)}(z - Z_k^b) \tag{23}$$

To assemble the total stiffness of the material we use the definition of force and moment resultants (Equations (6.11) in [17]). Therefore, the laminate constitutive equations become

$$\begin{bmatrix} N_x \\ N_y \\ N_{xy} \\ M_x \\ M_y \\ M_{xy} \end{bmatrix} = \begin{bmatrix} A_{11} & A_{12} & A_{13} & B_{11} & B_{12} & B_{13} \\ A_{12} & A_{22} & A_{23} & B_{12} & B_{22} & B_{23} \\ A_{13} & A_{23} & A_{33} & B_{13} & B_{23} & B_{33} \\ B_{11} & B_{12} & B_{13} & D_{11} & D_{12} & D_{13} \\ B_{12} & B_{22} & B_{23} & D_{12} & D_{22} & D_{23} \\ B_{13} & B_{23} & B_{33} & D_{13} & D_{23} & D_{33} \end{bmatrix} \begin{bmatrix} \varepsilon_x^0 - \varepsilon_x^p \\ \varepsilon_y^0 - \varepsilon_y^p \\ \gamma_{xy}^0 - \gamma_{xy}^p \\ \kappa_x - \kappa_x^p \\ \kappa_y - \kappa_y^p \\ \kappa_{xy} - \kappa_{xy}^p \end{bmatrix} \tag{24}$$

where the coefficients are computed in terms of the damaged values of the reduced stiffness coefficients in global coordinates $\bar{Q}^d_{i,j}$ using the standard equations (Equation (6.16) in [17]). Noting that the damage and unrecoverable effects are piecewise linear functions through the thickness of the laminate we obtain the following explicit equations for the coefficients of the laminate stiffness matrices

$$A_{ij} = \frac{1}{t_k}\left(\frac{\overline{Q^d_{ij}}(Z^t_k) + \overline{Q^d_{ij}}(Z^b_k)}{2}\right)(Z^t_k - Z^b_k)^2$$

$$\begin{aligned} B_{ij} &= \frac{1}{6}\frac{1}{t_k}\{(Z^t_k)^3[2\overline{Q^d_{ij}}(Z^t_k) + \overline{Q^d_{ij}}(Z^b_k)] + (Z^b_k)^3[\overline{Q^d_{ij}}(Z^t_k) + 2\overline{Q^d_{ij}}(Z^b_k)] \\ &\quad -3 \cdot Z^t_k Z^b_k[\overline{Q^d_{ij}}(Z^t_k)Z^t_k + \overline{Q^d_{ij}}(Z^b_k)Z^b_k]\} \\ D_{ij} &= \frac{1}{12}\frac{1}{t_k}\{(Z^t_k)^4[3\overline{Q^d_{ij}}(Z^t_k) + \overline{Q^d_{ij}}(Z^b_k)] + (Z^b_k)^4[\overline{Q^d_{ij}}(Z^t_k) + 3Q^d_{ij}(Z^b_k)] \\ &\quad -4Z^b_k Z^t_k[\overline{Q^d_{ij}}(Z^t_k)(Z^t_k)^3 + \overline{Q^d_{ij}}(Z^b_k)(Z^b_k)^3]\} \end{aligned} \tag{25}$$

INTERNAL MATERIAL CONSTANTS

The constitutive model developed in the previous sections involves a series of parameters that are material dependent and remain constant during the analysis, as follows: **J** and **H** are tensors that control shape of the damage and the potential surfaces, R_0 and γ are the damage and unrecoverable deformations thresholds c_1, c_2, C_1^p are the damage and unrecoverable hardening constants. Since both **J** and **H** are diagonal tensors, only eleven coefficients need to be found (only nine for plane stress). While several formulations exist for the **J** tensor [29], they involve a large number of parameters that, although increase the accuracy, significantly increase the complexity of parameter identification and consequent testing. With the addition of the **H** tensor, the damage surface can be written in stress space as the Tsai–Wu surface. In this way the coefficients in the **J** and **H** tensors can be uniquely obtained in terms of the strength values F_i of the unidirectional lamina, which for the most part are available in the literature.

Writing the g^d function for longitudinal uniaxial tension and compression, Equation (15) becomes

$$\begin{aligned} \sqrt{J_{11}\frac{\overline{C_{11}}}{\Omega_1^6}F_{1t}^2} + \sqrt{|H_1|\frac{\overline{C_{11}}}{\Omega_1^6}F_{1t}} = (\gamma^* + \gamma_0) = 1 \\ \sqrt{J_{11}\frac{\overline{C_{11}}}{\Omega_1^6}F_{1c}^2} + \sqrt{|H_1|\frac{\overline{C_{11}}}{\Omega_1^6}F_{1c}} = (\gamma^* + \gamma_0) = 1 \end{aligned} \tag{26}$$

Equation (26) represents a linear system in which F_{1t} and F_{1c} are the longitudinal compressive and tension stress of a single composite lamina, the values J_{11} and H_1 are the unknown quantities, while the quantities Ω_{1c} and Ω_{1t} are the critical tension and compression values of the integrity tensors. Comparing the Tsai–Wu criterion to the linear system Equation (26) at failure, we set $(\gamma^* + \gamma_0)$ equal to 1. Hence, there are two equations that allow us to solve for the two parameters J_{11} and H_1.

In the transverse direction the damage function Equation (15) reduces to

$$\sqrt{J_{22}\frac{\overline{C_{22}}}{\Omega_{2t}^6}F_{2t}^2} + \sqrt{|H_2|\frac{\overline{C_{22}}}{\Omega_{2t}^6}F_{2t}} = (\gamma^* + \gamma_0) = 1 \tag{27}$$

In this way it is possible to express J_{22} in function of H_2 by the following equation

$$J_{22} = \left(1 - \sqrt{|H_2|\frac{\overline{C_{22}}}{\Omega_{2t}^6}F_{2t}}\right)^2 \left(\frac{\overline{C_{22}}}{\Omega_{2t}^6}F_{2t}\right)^{-2} \tag{28}$$

Considering in-plane shear loading and Equation (15), we get the following equation

$$\sqrt{\left(\frac{J_{11}}{\Omega_1^4} + \frac{J_{22}}{\Omega_2^4}\right)\frac{2\overline{C_{66}}}{\Omega_{1s}^2\Omega_{2t}^2}F_6^2} + \sqrt{\left|\frac{H_1}{\Omega_{1s}^2} + \frac{H_2}{\Omega_{2s}^2}\right|\frac{2\overline{C_{66}}}{\Omega_{1s}^2\Omega_{2s}^2}F_6} = (\gamma^* + \gamma_0) = 1 \tag{29}$$

Here F_6 value is the shear strength for a single composite lamina, while Ω_{1s} and Ω_{2s} are critical values of the integrity tensor at failure for a state of in-plane shear stress. Since the shear response of a fiber-reinforced lamina in material directions is independent of the sign of the shear stress, the coefficient of the linear term in F_6 of Equation (29) must be zero, leading to a relationship between H_1 and H_2, namely

$$\frac{H_1}{\Omega_{1s}^2} + \frac{H_2}{\Omega_{2s}^2} = 0 \Rightarrow H_2 = -\frac{\Omega_{2s}^2}{\Omega_{1s}^2}H_1 = -r_s H_1 \tag{30}$$

where $r_s = (\Omega_{2s}/\Omega_{1s})^2$ is an intermediate constant. Then H_2 can be written as a function of the r_s, and Equation (29) becomes

$$\sqrt{\frac{J_{11}r_s}{k_s}+\frac{J_{22}}{k_s r_s}\frac{2C_{66}}{k_s}}F_6^2=(\gamma+\gamma_0)=1;\quad k_s^2=\Omega_{1s}^2\Omega_{2s}^2=G_{12}^*/\overline{G_{12}} \tag{31}$$

where G_{12}^* is the unloading damaged shear modulus prior to imminent failure (e.g., last unloading curve in Figure 1). Since J_{11} is known from Equation (26) and k_s^2 is a known constant (see section Critical Damage Parameters), using Equations (28) and (31), it is possible to determine J_{22} and H_2. Thus, all the coefficients in the tensors $\mathbf{J}$ and $\mathbf{H}$ are found in terms of known parameters F_i and Ω_i.

CRITICAL DAMAGE PARAMETERS

The critical integrity parameters Ω_i introduced in the previous section represent the values of the integrity components when the material is near failure. They can be evaluated by formulas based on experimental results and analytical procedures.

In a pure in-plane shear test, and using Equation (3), the unloading shear stress–strain path just prior to failure (Figure 1) can be described in terms of either the damaged or the undamaged (i.e., virgin) shear stiffness as

$$\overline{\sigma}_6=2\overline{G_{12}}\Omega_{1s}\Omega_{2s}\varepsilon_6'=2G_{12}^*\Omega_{1s}^{-1}\Omega_{2s}^{-1}\varepsilon_6';\quad \varepsilon_6'=\varepsilon_6-\varepsilon_6^p \tag{32}$$

which defines the known coefficient k_s used in Equation (31) in terms of experimental data. In this way, the product of Ω_{1s}^2 and Ω_{2s}^2 represents the ratio between the damaged shear modulus (unloading) at imminent failure and the virgin state value, both of which can be determined by experimental in-plane shear data for a unidirectional composite lamina.

On the longitudinal direction, the probability of failure of a fiber in a composite lamina can be expressed by the Weibull statistic distribution [30]. The probability for unbroken fibers is

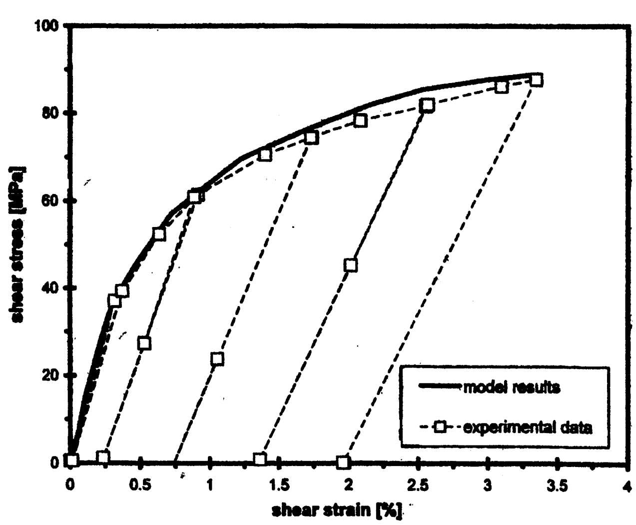

Figure 1. Cyclic shear behavior of unidirectional T300/915 Carbon/Epxoy.

$$P_u = 1 - F(\sigma) = 1 - \exp\left[-\frac{\delta}{L_0}\left(\frac{\sigma}{\sigma_0}\right)^m\right] \tag{33}$$

where $0 < P_u < 1$, σ is the stress in the unbroken fibers, δ is the shear lag length, L_0 is the length of the test fiber used to obtain the Weibull parameters σ_0 and m, which represent the dispersion of fiber strength. The bundle stress is $\sigma_b = P_u\sigma$. At fracture, the bundle stress σ_b has a maximum. Solving for the fiber stress σ, the critical value of fiber stress is

$$\sigma_c = \sigma_0\left(\frac{\delta_m}{L_0}\right)^{-1/m} \tag{34}$$

The bundle strength can be found by substituting Equation (34) back into $\sigma_b = P_u\sigma$. The critical damage D_{1t} at fracture is the ratio of broken to original fiber area, which is found from Equations (33) and (34) as

$$D_{1t} = 1 - \exp\left(\frac{-1}{m}\right) \tag{35}$$

The Weibull dispersion parameter is available from the literature for most types of fibers [34,35,37].

For longitudinal compression, the damage critical value can be evaluated according to the microbuckling and misalignment of the fiber. Fiber misalignment, which is strongly dependent on processing conditions and can be considered as an inherent defect, increases the possibility for the fiber to buckle. For each misalignment angle θ, the composite area-fraction with buckled fiber $\omega(\theta)$ corresponding to fibers with misalignment angle greater than θ, can be taken as measure of damage. Since the fiber misalignment distribution is Gaussian, the critical compressive damage D_{1c} is

$$D_{1c} = \omega(\theta^*) = 1 - \mathrm{erf}\left(\frac{\theta^*}{\Lambda\sqrt{2}}\right) \tag{36}$$

where erf(−) is the error function, Λ the standard deviation of the actual Gaussian distribution of fiber misalignment, and θ^* is the critical misalignment angle at failure [31,32]. The value of Λ can be measured experimentally [33] or computed in terms of experimental values for F_{1c}, F_6 and G_{12} using Equations (4.74)–(4.75) in [17].

In the transverse direction, it is possible to think of the matrix as a periodic link structure enclosed between fibers. Assuming a constant probability distribution for the failure of the matrix link it is possible to derive the maximum admissible strength for the bundle matrix [5]. The ratio between the broken links and the initial ones can be considered a measure of damage. Therefore, the critical damage value is

$$D_{1c} = \frac{1}{2} \tag{37}$$

MODEL IDENTIFICATION AND VALIDATION

Unidirectional lamina experimental data for two materials, Aramid/Epoxy and Carbon/Epoxy are used to obtain all the parameters required in the model [2]. Laminate and off-axis experimental data for the same materials is then used to demonstrate the predictive capabilities of the proposed model.

In-plane shear experimental data of unidirectional composite in Figure 1 is used to adjust the model parameters for Carbon/Epoxy T300/915. The material properties are given in Table 1. The intermediate parameters, determined completely in terms of the material properties are given in Table 2. The adjustable model parameters, determined with the aid of the shear stress–strain plot, are given in Table 3. The model is used to predict the amount of unrecoverable strain, and the results are compared with experimental data in Figure 2. The predicted damage evolution is shown in Figure 3. Failure is predicted to occur when the transverse damage d_2 equals the critical value D_{2t}, as shown in Figure 3. In the actual test, the sample failed at about 3% shear strain, in good agreement with the predicted value of strain at failure. Next, the model is used to predict

Table 1. Material properties.

Property	Carbon/Epoxy T300/915	Aramid/Epoxy
E_1(GPa) undamaged	142.0	73.4
E_2(GPa) undamaged	10.3	5.5
G_{12}(GPa) undamaged	7.29	3.65
G_{12}(GPa) damaged	3.71	2.21
ν_{12} undamaged	0.27	0.34
F_{1t}(MPa)	1839	1137.1
F_{1c}(MPa)	1096	212.5
F_{2t}(MPa)	57	27
F_{2c}(MPa)	57	27
F_6(MPa)	86	47

Table 2. Intermediate parameters univocally determined in terms of the material properties given in Table 1.

Property	Carbon/Epoxy T300/915	Aramid/Epoxy
J_{11}	$0.2523910783 \times 10^{-14}$	$0.4647013345 \times 10^{-13}$
J_{22}	$0.1166642654 \times 10^{-12}$	$0.1380462161 \times 10^{-12}$
J_{33}	0	0
H_1	$0.1297694304 \times 10^{-7}$	$0.7518017147 \times 10^{-6}$
H_2	$-0.75544663738 \times 10^{-8}$	$-0.3245140897 \times 10^{-6}$
H_3	0	0
k_s	0.515	0.605
r_s	0.581	0.416

Table 3. Model parameters.

Property	Carbon/Epoxy T300/915	Aramid/Epoxy
c_1	0.17	0.1
c_2	-8.9×10^5	-4.0×10^5
γ_0	-0.2	-0.3
c_1^p	1.2×10^{-6}	1.5×10^{-6}
R_0	0.25	0.5

the monotonic loading behavior of a $[45/-45]_{2s}$ laminate, which compares favorably with cyclic experimental data in Figure 4. Comparison between predicted and measured unrecoverable strain versus total shear strain is shown in Figure 5. Comparison between predicted and measured axial stiffness versus total axial strain of a $[45/-45]_{2s}$ is shown in Figure 6.

Experimental data for unidirectional Aramid/Epoxy loaded with cyclic in-plane shear is used to adjust the model parameters, as shown in Figure 7. The model is then used to predict the amount of unrecoverable strain, and the results are compared with experimental data in Figure 8. The predicted damage evolution is shown in Figure 9.

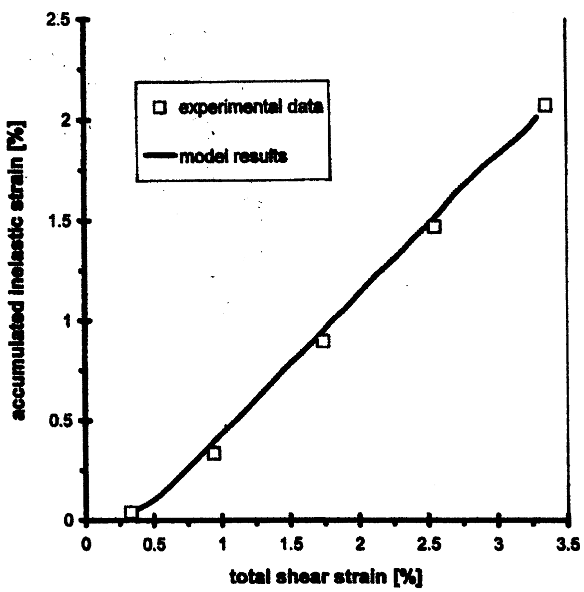

Figure 2. Accumulated unrecoverable strain of unidirectional T300/915 Carbon/Epoxy under shear loading.

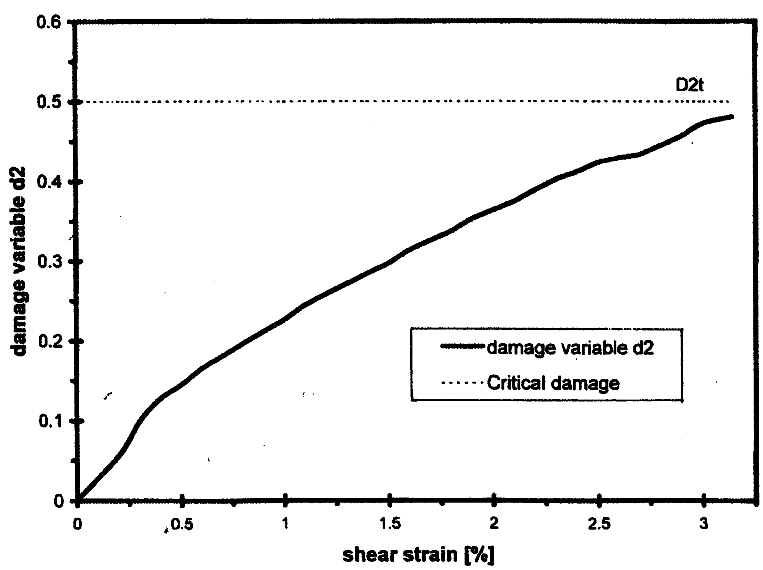

Figure 3. Damage evolution up to failure of unidirectional T300/915 Carbon/Epoxy under shear loading.

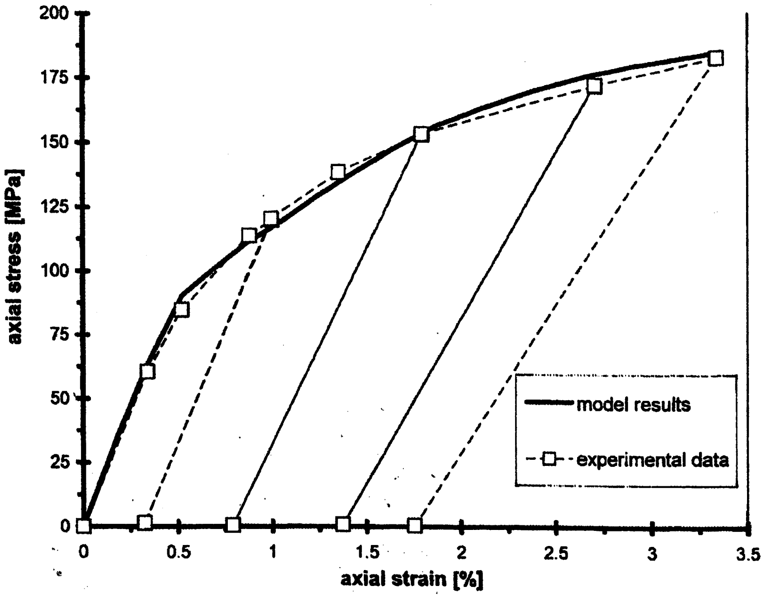

Figure 4. *Comparison with experimental axial behavior of [45|−45]$_{2s}$ T300/915 Carbon/Epoxy.*

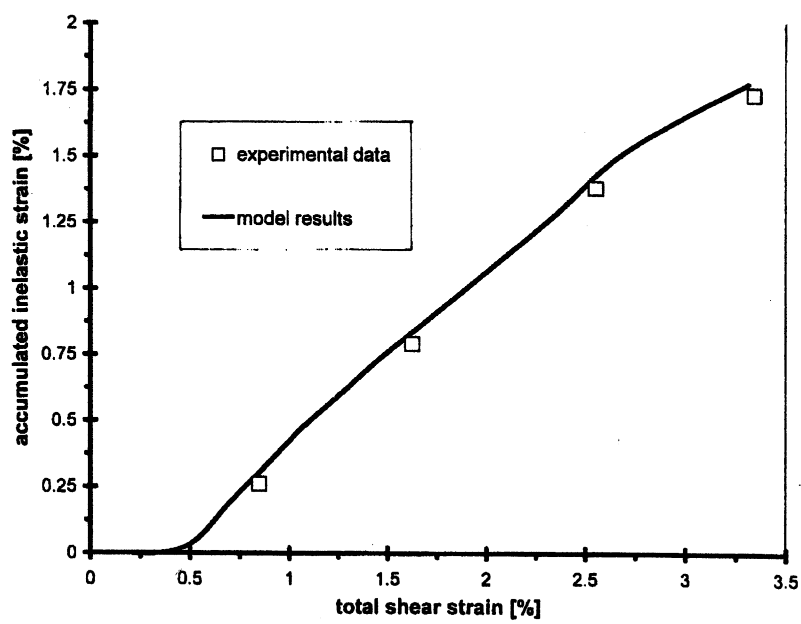

Figure 5. *Comparison with experimental accumulated unrecoverable strain in [45/−45]$_{2s}$ T300/915 Carbon/Epoxy.*

The Aramid/Epoxy failed in shear at about 3% shear strain, when the predicted longitudinal damage d_l is 90% of the critical value $D_{1c}=0.114$. Next, the model is used to predict the monotonic loading behavior of a 10° off-axis lamina, which compares favorably with cyclic experimental data in Figure 10. Also, the model is able to accurately predict the accumulated unrecoverable strain of the 10° off-axis test, as shown in Figure 11.

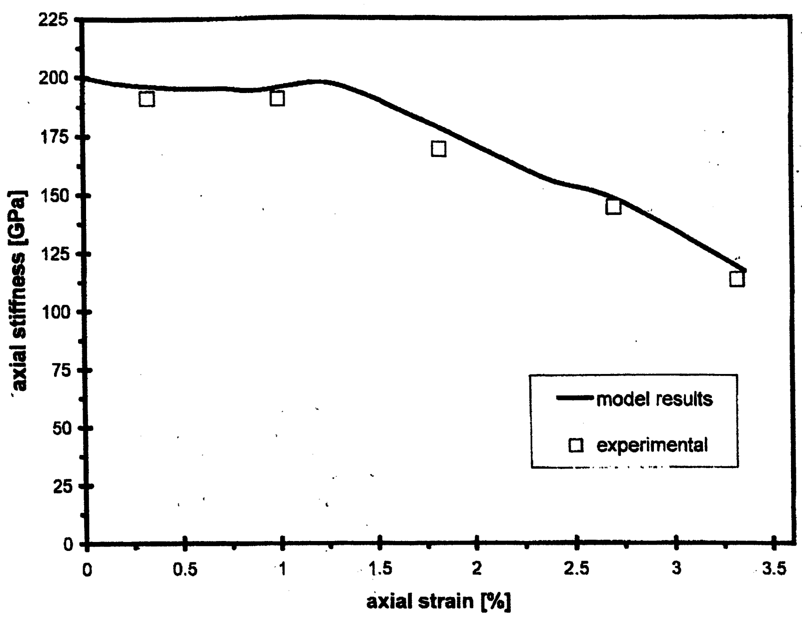

Figure 6. Comparison with experimental reduced stiffness of $[45/-45]_{2s}$ T300/915 Carbon/Epoxy.

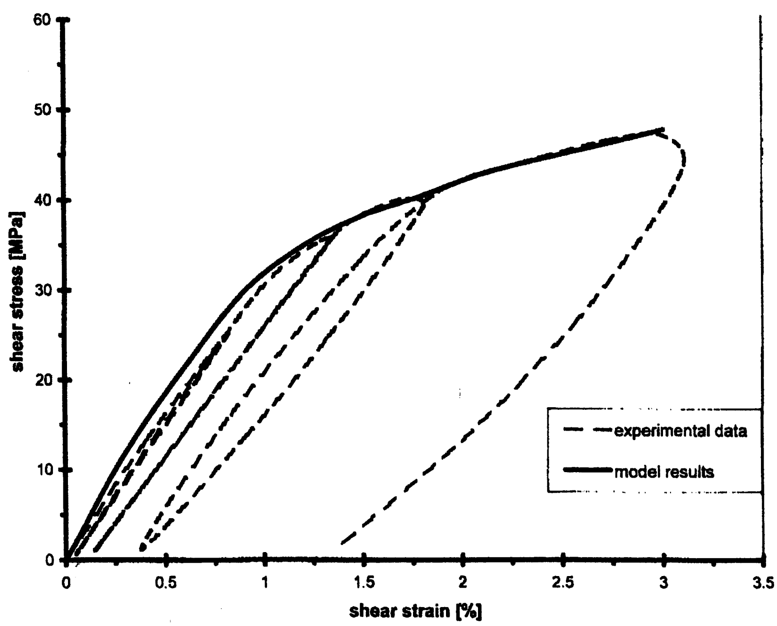

Figure 7. Cyclic shear behavior of unidirectional Aramid/Epoxy.

SUMMARY

The procedure used to adjust the model parameters is summarized in this section. The model parameters describe damage and unrecoverable deformation respectively.

The damage evolution parameters c_1, c_2 control the damage evolution by Equation (10). The damage threshold γ_0 represents the initial size of the damage surface. No damage can occur until the thermodynamic forces $\mathbf{Y}$ reach the damage surface. These three parameters

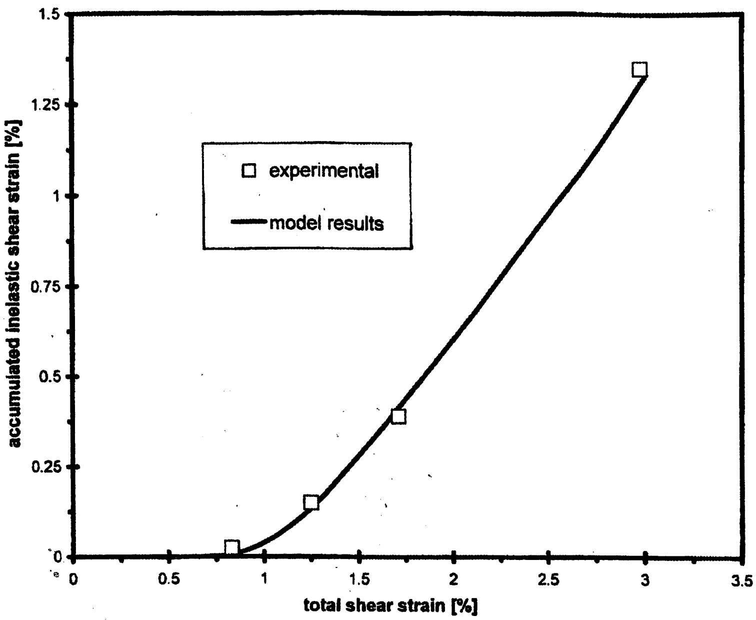

Figure 8. *Accumulated unrecoverable strain of unidirectional Aramid/Epoxy under shear loading.*

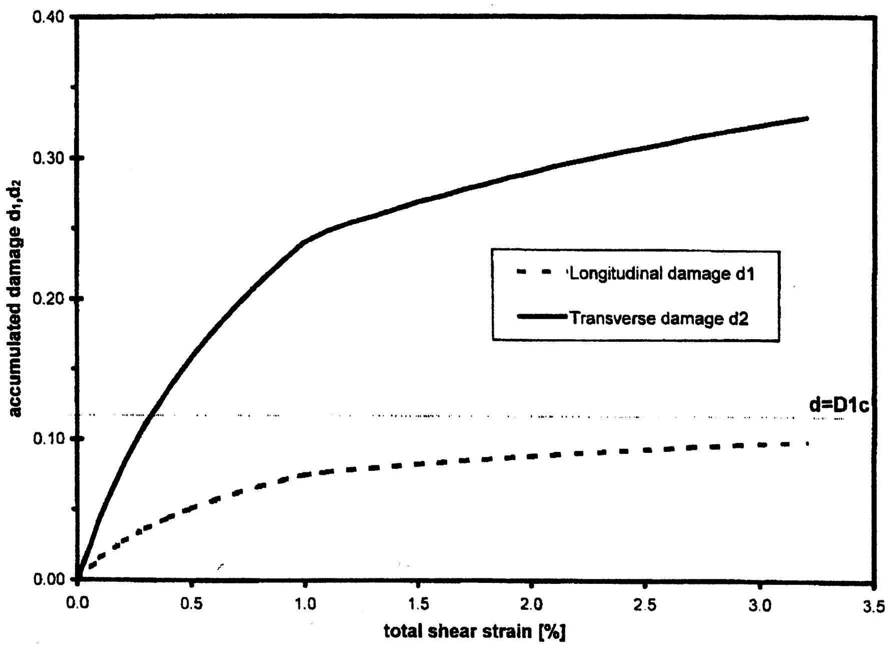

Figure 9. *Damage evolution up to failure of unidirectional Aramid/Epoxy under shear loading*

are adjusted with the monotonic loading part of the shear stress–strain diagram, such as the top curve in Figure 1.

The unrecoverable deformation parameter c_1^p controls the evolution of unrecoverable strain. The threshold parameter R_0 represents the initial size of the unrecoverable deformation surface (yield surface). These two parameters are adjusted with the experi-

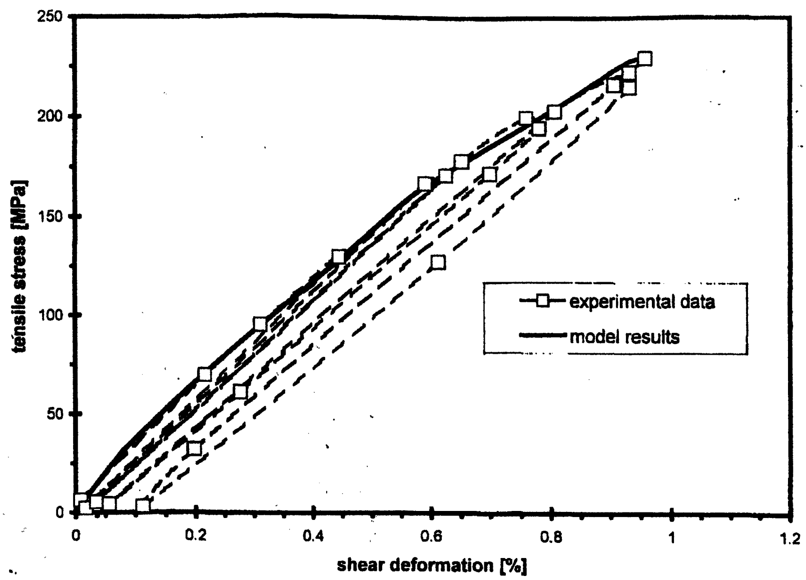

Figure 10. Comparison with experimental axial behavior of 10° off-axis test of Aramid/Epoxy.

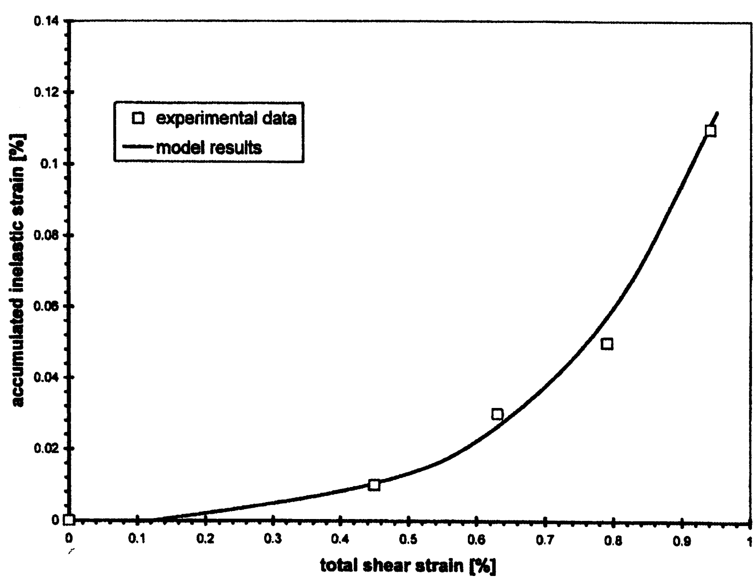

Figure 11. Comparison with experimental accumulated unrecoverable strain of 10° off-axis test of Aramid/Epoxy.

mental unrecoverable deformations resulting from unloading, such as those read from unloading in Figure 1 and plotted in Figure 2.

The influence of these parameters on the predictions is discussed next, using T300/915 material as an example. The performance of the model is measured by the χ^2 statistical measure of the difference between the predicted values p_i and the experimental values e_i during an appropriate test over which the values have significant influence. The statistical measure is defined as follows

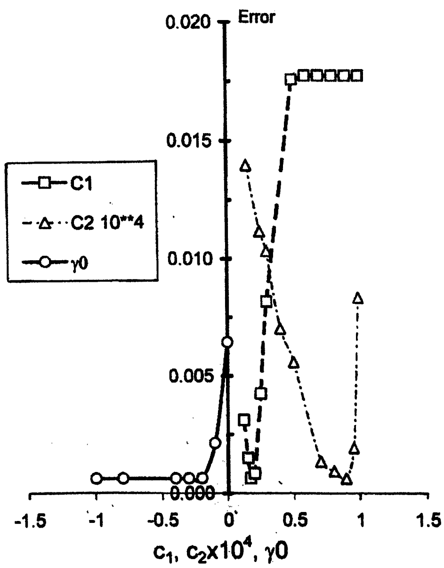

Figure 12. *Sensitivity of results to changes in the damage evolution parameters c_1, c_2, γ_0.*

$$\chi^2 = \frac{\sum (p_i - e_i)^2}{\sum e_i^2} \tag{38}$$

First, the damage evolution parameters (c_1, c_2, γ_0) are varied within one order of magnitude around the optimum values previously determined in the preceding section, while keeping the unrecoverable deformation parameters fixed. Equation (38) is used to evaluate the error in predicting the loading portion of the shear stress–strain curve (e.g., top curve in Figure 1). It can be seen in Figure 12 that the error of the prediction, as measured by Equation (38), has a minimum for the optimum values of c_1 and c_2. Any deviation from those values results in a clear loss of accuracy.

From Equations (10) and (15), setting the damage threshold $\gamma_0 < -c_1$ starts damage immediately ($\delta = 0$). Larger values can be used to delay the onset of damage when it is necessary, but for T300/915, damage must start immediately in order to yield curvature to the stress–strain loading curve from the onset of loading, as shown in Figure 1.

Keeping the damage evolution parameters fixed, the unrecoverable deformation parameters (c_1^p, R_0) were varied within one order of magnitude around the optimum values previously determined in the preceding section. Equation (38) is used to evaluate the error in predicting the unrecoverable deformations (e.g., Figure 2). It can be seen in Figure 13 that the error of the prediction, as measured by Equation (38), has a minimum for the optimum value of c_1^p The unrecoverable deformation threshold R_0 controls when unrecoverable deformations start accumulating (see Figure 2).

The internal material constants J_{11}, J_{22}, H_1, H_2, r_s, and k_s are used to write the model equations in a concise form. These are not adjustable model parameters since their values are univocally determined in terms of the available material constants F_{1t}, F_{1c}, F_{2t}, F_{2c}, F_6, G_{12}^* (see section Internal Material Constants) and the critical damage values D_{1t}, D_{1c}, D_{2t} (see section Critical Damage Parameters). The latter are fixed values in terms of material constants m and Λ as described by Equations (35)–(37). The Weibull dispersion of fiber strength m and the misalignment angle Λ are available from the literature [9,34,35,37] and

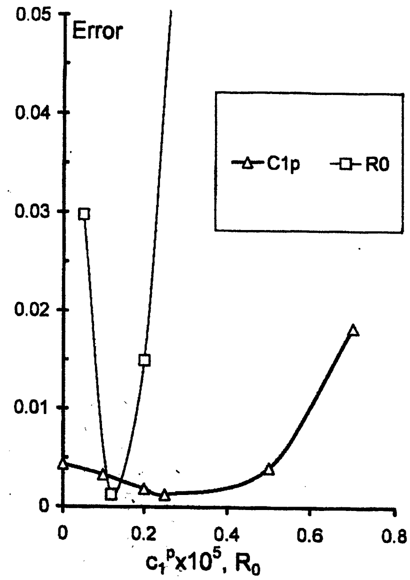

Figure 13. Sensitivity of results to changes in the unrecoverable deformation evolution parameters c_1^p, R_o.

well-established procedures exist to measure them for new materials [33,36]. Finally, the material constants E_1, E_2, G_{12}, and ν_{12} are readily available. The only information that is not readily available is the shear stress–strain plot, as in Figure 1. The loading part of the plot is necessary to adjust the damage evolution parameters (c_1, c_2, γ_0). The unloading part of the plot is necessary to adjust the unrecoverable deformation evolution parameters (c_1^p, R_0). Such a plot can be determined experimentally using a shear test fixture such as described in ASTM D5379.

CONCLUSIONS

The proposed model predicts the damage and unrecoverable deformations phenomena of a laminated composite material under proportional loading. A limited number of internal variables are used in the model to represent the evolution of the damage and unrecoverable deformations phenomena. Comparisons between experimental data and model predictions are good in terms of damage and unrecoverable deformations evolution. Some further development and improvements are envisioned to account for closure during unloading. Also, further validation would be useful as additional low-cycle stress–strain data becomes available.

REFERENCES

1. Aboudi, J. (1991). *Mechanics of Composite Materials: A Unified Approach.* Elsevier.
2. Herakovich, C.T. (1988). *Mechanics of Fibrous Composites.* N.Y: John Wiley.
3. Chaboche, J.L. (1993). Development of CDM for elastic solids sustaining anisotropic and unilateral damage. *International Journal of Damage Mechanics*, **2**(4): 311–317.
4. Ladeveze, P. and LeDantec, E. (1992). Damage modelling of the elementary ply for laminated composites. *Composites Science and Technology*, **43**: 257–267.
5. Krajcinovic, D. (1996). *Damage Mechanics.* Holland, Amsterdam; North Holland Pub.

6. Voyiadjis, G.Z. and Deliktas, B. (2000). A coupled anisotropic damage model for the inelastic response of composite materials. *Comp. Methods in Appl. Mech. Eng.*, **183**: 159–199.
7. Kachanov, L.M. (1958). On the creep fracture time. *Izv. Akad Nauk USSR Otd.Tekh.*, **8**: 26–31.
8. Kachanov, L.M. (1992). Effective elastic properties of cracked solids: critical review of some basic concepts. *Appl. Mech. Rev.*, **45**(8): 304–335.
9. Wen, E. (1999). Compressive strength prediction for composite unmanned aerial vehicles. Thesis, West Virginia University, Morgantown, WV.
10. Barbero, E.J. and Wen, E. (2000). Compressive strength of production parts without compression testing. *Composite Structures: Theory and Practice*. ASTM STP 1383, ASTM, PA, 470–483.
11. Piggott, M.R., Liu, K. and Wang, J. (2000). New experiments suggest that all the shear and some tensile failure processes are inappropriate subjects for ASTM standards. *ASTM STP Composite Structures: Theory and Practice*.
12. Chaboche, J.L. (1984). Anisotropic creep damage in the framework of continuum damage mechanics. *Nuclear Eng. and Design*, **79**: 309–319.
13. Lubarda, V.A. and Krajcinovic, D. (1993). Damage tensors and cracks density distribution. *Int. J. Solids Structures*, **30**: 2859–2877.
14. Ogden, R.W. (1984). *Non-Linear Elastic Deformation*. Mineola, NY: Dover Publications, Inc.
15. Barbero, E.J. and De Viro, L. (2001). A Constitutive Model for Elastic Damage in Fiber Reinforced PMC Laminae, *J. of Damage Mechanics*, **10**(1): 73–93.
16. Marsden, H. (1983). *Mathematical Foundation of Elasticity*. Englewood Cliffs, NJ: Prentice Hall Inc..
17. Barbero, E.J. (1999). *Introduction to Composite Materials Design*. Philadelphia, PA; Taylor & Francis.
18. Trusdell, C. (1966). *The Elements of Continuum Mechanics*. New York: Springer-Verlag.
19. Coleman, B.D. and Gurtin, M.E. (1967). Thermodynamics with internal state variables. *J. Chem. Phys.*, **47**: 597–613.
20. Lubliner, J. (1972). On the thermodynamic foundations of nonlinear solids mechanics. *Int. J. Non-Linear Mech.*, **7**: 237–254.
21. Chow, C.L. and Wang, J. (1987). An anisotropy theory of elasticity for continuum damage mechanics. *Int. J. Fracture*, **33**: 3–16.
22. Cordebois, J.L. and Sirodoff, F. (1979). Damage Induced Elastic Anisotropy, Colloque Euromech 115, Villard de Lans, France.
23. Barbero, E.J. and Lonetti, P. (2001). Damage Model for Composites Defined in Terms of Available Data, *J. Mechanics of Composite Materials and Structures*, **8**(4): 299–316.
24. Strang, G. (1986). *Introduction to Applied Mechanics*. Wellesley, MA: Wellesley-Cambridge.
25. Chow, C.L. and Wei, Y. (1991). A model of continuum damage mechanics for fatigue failure. *Int. J. Fracture*, **50**: 301–316.
26. Hansen, N. and Schreyer, H.L. (1994). A thermodynamic consistent framework for theories of elastoplasticity coupled with damage. *Int. J. Solids Structures*, **31**: 359–389.
27. Schwartz, M.M. (1997). *Composite Materials: Properties, Non-destructive Testing, and Repair*. NJ: Prentice Hall.
28. ASTM Standards (2000). High Modulus Fibers and Composites, v15.03.
29. Chow, C.L. and Lu, T.J. (1989). On the evolution laws of anisotropic damage. *Eng. Fracture Mechanics*, **34**(3): 679–701.
30. Kelly, K. (1993). The effect of fiber damage on longitudinal creep of a CFMMC. *Int. J. Solids Structures*, **30**: 3417–3429.
31. Barbero, E.J. (1998). Prediction of compression strength of unidirectional polymer matrix composites. *Journal of Composites Material*, **32**(5): 483–502.
32. Barbero, E.J. and Tomblin, J. (1996). A damage mechanics model for compression strength of composites. *Int. J. Solids Structures*, **33**: 4379–4393.

33. Yurgartis, S.W. and Sternstein, S.S. (1992). Experiments to reveal the role of matrix properties and composite microstructure in longitudinal compression response of composite structures. ASTM, 16–17 Nov.
34. McDonough, W.G. and Clough, R.B. (1996). The measurement of fiber strength parameters in fragmentation tests by using acoustic emissions. *Composite Science and Technology*, **56**: 1119–1127.
35. Schultheiz, C.R., McDonough, W.G., Shrikant, K., Shutte, C.L., Mcturk, K.S., McAulife, M. and Hunston, D.L. *13th Symposium on Composites Testing and Design*, ASTM, PA. pp. 257–286.
36. Kasai, Y. and Saito, M. (1979). Weibull analysis of strengths of various reinforcing filaments. *Fibre Science and Technology*, **12**: 21–29.
37. Haberle, J.G. (1991). Strength and failure mechanisms of unidirectional carbon fibre-reinforced plastics under axial compression. PhD Thesis, Imperial College, London, U.K.